Mouse lemur, a new primate model to investigate cardiac pacemaker activity.

Mattia L. DiFrancesco[1,2,4-5], Romain Davaze[3], Eleonora Torre[1,2], Pietro Mesirca[1,2], Manon Marrot[1,2], Corinne Lautier[6], Pascaline Fontes[6], Joël Cuoq[6], Anne Fernandez[3], Fabien Pifferi[7], Nadine Mestre-Francés[6,8], Matteo E. Mangoni[1,2] and Angelo G. Torrente[1,2].

[1]Institute of Functional Genomics, Univ. Montpellier, CNRS, INSERM, Montpellier, F-34095, France.
[2]LabEx Ion Channels Science and Therapeutics (ICST).
[3]Cell Biology group, Institute of Human Genetics, CNRS and Univ. Montpellier, Montpellier, F-34095, France.
[4]Center for Synaptic Neuroscience, Istituto Italiano di Tecnologia, Largo Rosanna Benzi 10, 16132 Genova, Italy.
[5]IRCCS Ospedale Policlinico San Martino, Genova, Italy.
[6]MMDN Univ. Montpellier, Montpellier, F-34095, France.
[7]UMR CNRS/MNHN 7179, Mécanismes Adaptatifs et Evolution, Brunoy, France
[8]EPHE, PSL Research University, Paris, France

Corresponding authors:

Dr. Matteo E. Mangoni and Angelo G. Torrente

Institute of Functional Genomics, Department of Physiology
CNRS UMR 5203, INSERM U 1191, University of Montpellier
34097 Montpellier, France
tel. +33 (0)4 34 35 92 46
e-mail: matteo.mangoni@igf.cnrs.fr and angelo.torrente@igf.cnrs.fr

Abstract

The mouse lemur (*Microcebus murinus*) is one of the most ancestral primates known so far and has a size that lay in between those of mice and rats. Thanks to its genetic proximity to humans, it is an emerging model of senescence and neurodegeneration. Equally, this primate could improve understanding of cardiac physiology in human, but this topic has not been investigated yet in this animal.

Here we characterize cardiac activity in mouse lemurs, focusing on the generation of pacemaker activity by the Sinoatrial node (SAN). Notably, we recorded cardiac activity in animals, isolated hearts, atrial preparations and SAN pacemaker myocytes. This revealed that accordingly to their size, the heart rate of mouse lemurs lays in between those of mice and rats. However, the ventricular depolarization of these lemurs is more similar to humans or large mammals than it is to small rodents.

In the myocytes isolated from the lemurian sinoatrial node we recorded three of the main ionic currents involved in the vertebrate pacemaker activity: I_f, $I_{Ca,L}$ and $I_{Ca,T}$, and the expression of the sinoatrial node marker HCN4.

In parallel, we characterized skeletal muscle-derived stem cells (MDSCs) from *M. murinus*. These stem cells differentiate *in vitro* into pacemaker-like (PML) cells that showed common features with native SAN pacemaker myocytes and could be useful to test pharmacological strategies to modulate pacemaker activity.

In conclusion, our characterization of *M. murinus* pacemaker activity, together with the generation of PML cells pave the way for comparative studies of cardiac physiology in primates and pharmacologic tests to tackle diseases of cardiac automaticity.

Introduction

The sinoatrial node (SAN) is the natural pacemaker of the heart[1,2]. This tissue is situated at the venous inflow of the right atrium and it is enriched in spindle shaped cells that depolarize spontaneously to generate the cardiac impulse[3]. The pacemaker activity of the SAN sets the intrinsic frequency of heart rate, which is constantly modulated by the autonomic nervous system to determinate the resting heart rate[4,5]. We recently had the opportunity to undertake a pilot study of cardiac pacemaker activity on the small mouse lemur *Microcebus murinus.* To our knowledge, this is the first detailed characterization of cardiac pacemaker activity in primates. Given the close genetic heritage with our species[6,7], this animal model could help translate results from fundamental cardiac research to clinical approaches to treat patients affected by dysfunction of SAN pacemaker activity.

Dysfunctions of SAN pacemaker activity causes various pathologies that are strongly related to ageing[8]. These pathologies cause about half of the 500k electronic pacemakers that are implanted every year in Europe[9], at a cost of ~2 Billion $[10]. Due to societal aging, SAN dysfunctions are emerging as a family of pathologies that urgently need alternative therapies, other than classical implantation of electronic pacemakers[11 12]. Indeed, while these electronic devices are very performant, they are expensive, require a long term follow up and every 7 to 10 years the change of their batteries can cause infections that impede the reimplantation, leaving the patient under a life-threatening risk during the convalescence period.

With the ultimate objective to develop alternative therapies against SAN dysfunctions, several studies have investigated the fundamental mechanism of SAN pacemaker activity[13 14 15]. It is very difficult to study living human hearts and monkey samples are hard to obtain and raise strong ethical concerns. So, only few studies of pacemaker activity have been conducted on the taxonomic order of primates[16 17 18]. Because of this most SAN research has been pursued in rodents. In particular, with the arrival of transgenic mice, that species prevailed and allowed to discriminate the implication of specific proteins in SAN pacemaker activity[3,19].

Pacemaker activity of SAN myocytes is an electric phenomenon that involves ion flow through the plasma-membrane in a yet unclear way. However, it is generally agreed that functional association between plasma membrane ionic channels and intracellular Ca^{2+} dynamics generate the currents necessary to spontaneously depolarize SAN myocytes[20]. In particular, hyperpolarization-activated "funny" f-(HCN) channels and L-type and T-type Ca^{2+} channels generate the main depolarizing current of the plasma-membrane, while the interaction between Ca^{2+} release from the Ryanodine Receptors and Na^{+}/Ca^{2+} exchange (NCX) generates the inward current resulting from the intracellular Ca^{2+} dynamics[20].

While considerable evidence of the role of these currents has been collected mainly in rodents, their relative contribution to diastolic depolarization in humans is still debated due to the reduced data obtained with SAN cells from patients[21]. Indeed, although SAN pacemaker activity in mice reproduces quite well the equivalent physiology in humans[22 23 14], the genetic distance between rodents and humans must be taken into consideration.

This justifies the exploration of new species, genetically closer to humans, like *M. murinus* to study cardiac pacemaker activity. *M. murinus* is a very small and ancestral primate that typically lives 4 to 5 years in the wild, but can live up to 12 years in captivity, undergoing a period of prolonged ageing like human patients. In captivity, it is bred because, unlike rodents and similarly to humans, it spontaneously develops age-related neurodegeneration like Alzheimer disease[24 25 26 27 28]. Moreover, it presents unique and ancestral features for primates, like the ability to enter into a torpor state to save energy when the outside temperature drops[29 30].

Common genetic origins with our species[6,7] and adequate growing and reproduction rates, make mouse lemurs an excellent animal model for pacemaker research. Here we investigate for the first time the mouse lemur's potential for cardiovascular research.

In mammals, the frequency of heart contractions is determined by the body size of the animals, in order to sustain physiological and metabolic needs[31 32]. Given that mouse lemurs have an average weight of 60-90 g and a body length of 12-14 cm[33], we compared our findings on *M. murinus* with previous results in mammals of similar sizes, such as rats and mice. When possible and relevant, we also compared cardiac activity in mouse lemurs and humans.

For this purpose, we characterized cardiac pacemaker activity of mouse lemurs i) in freely moving and anaesthetized animals, ii) in isolated heart and atrial preparations, and iii) in single SAN pacemaker myocytes. In addition, we used biopsies of skeletal muscle from *M. murinus* to isolate skeletal muscle-derived stem cells (MDSCs) that differentiate *in vitro* into automatic cells showing a pacemaker-like (PML) phenotype similar to native pacemaker myocytes of the SAN, as we have previously reported in rodents[34,35].

This study documents heart rate, ionic currents and the differentiation of PML cell from *M. murinus*. Thus, it paves the way for future cardiovascular studies on small primates and to an easier translation of results from fundamental cardiovascular research to clinical application.

Results

1. Analysis of heart rate in freely moving and anaesthetized mouse lemur.

We equipped mouse lemurs of 1 to 5 years of age with subcutaneous telemetric transmitters to record electrocardiograms. This technique allowed us to discern P waves corresponding to atrial contraction and the subsequent QRS complex and T waves, which correspond to ventricles depolarization and repolarization, respectively (Fig. 1A). Analysing the electrocardiogram recordings in one lemur for 22 h we detected the main range of heart rate between 200 and 500 beat per min (bpm; Fig. 1B). This heart rate is similar to the frequency reported for the rodents of closer size, mice and rats, respectively[36 37]. Thus, it is consistent with the body size of *M. murinus*. In addition, in graphical representation of heart rate along the time in two mouse lemurs, we observed gradual slowdown of heart rate to 200 or less bpm from an average of 300 to 400 bpm. These slowdowns occurred repeatedly and were often followed by sudden heart rate increases (Fig. 1C, D and E). The analysis of heart rate variability along the time revealed that these heart rate decrease happened with a slow dynamic that impacted more the indexes of long-term variability (coefficient of variability of the RR interval between successive heartbeats), rather than the short-term variability [root mean square of successive differences between heart beats intervals (RMSSD); Fig 1D]. We obtained similar results analysing long- and short-term indexes of heart rate variability derived from Poincaré analysis (Suppl. Fig. 1). Thus this phenomenon appears different from the short and physiological heart rate decrease determined by fast intracellular release of acetylcholine in SAN pacemaker myocytes[5].

In the electrocardiogram of *M. murinus* we recorded well visible T waves separated from the QRS complexes by short isoelectric ST segments (Fig. 1 A). These T waves are remarkably different from those of small rodents and more similar to those of large mammals[38] and humans[36 39].

Next, we used external device to obtain shorter recording of heart rate in *M. murinus* during animal handling, which likely cause positive autonomic modulation of cardiac activity. This method revealed an average heart rate of 500 ± 31 bpm (n=3) versus the average rate of 427 ± 43 bpm (n=4) recorded in freely moving animals equipped with subcutaneous electrocardiogram devices (Fig. 2A and B).

We repeated electrocardiogram recording also in anaesthetized animals, which allows to record cardiac activity under reduced autonomic modulation of heart rate (Fig 2C and D). The average heart rate determined by this condition was 372 ± 27 bpm (n=5), which according to *M. murinus* body size again places it between mice and rats[36 40]. Interesting, also on these recordings of anaesthetised mouse lemurs, we highlighted clear T waves slightly separated from QRS complexes as in freely moving animals.

2. Analysis of intrinsic pacemaker activity by Langendorff perfusion of the whole heart and voltage optical mapping of atrial preparations.

To comply with the "three R's" of animal welfare we obtained results on isolated cardiac tissue of *M. murinus* only from animals of 6 to 11 years that have been used for other studies and that natural ageing entailed to be euthanized for factors that hamper normal life. Thanks to these animals, we recorded electrocardiogram signals from isolated hearts, obtained after deep anaesthesia of the animals and complete loss of hind-limb reflex, indicative of cerebral death. After removal, the hearts of these animals were placed on a Langendorff perfusion system that maintained a robust and regular heart rate of 232 ± 80 bpm (Fig. 3 A).

In other hearts, we investigated pacemaker activity by analysing the intact atrial preparation, after removal of ventricular chambers. These preparations include the SAN and the right and left atria. In *M. murinus* these preparations are about twice the size of those observed in mice of equivalent ages (Fig 3B). Moreover, differently from mice, where the size of the right atria is slightly larger than the left atria, in *M. murinus* the size of left atria is significantly larger than right atria (Supp. fig.1).

Thanks to the technique of voltage optical mapping, we next recorded the rate of action potentials (APs) in the SAN region of both *M. murinus* and mice, as well as the localization of the first electrical activity in the SAN and the conduction of the electrical impulse towards the atria (Fig 3B, C, D and E and Suppl. Video 1). We reported an average pacemaker frequency of 236 ± 18 APs/min, which is

similar to what we recorded in Langendorff perfused hearts and significantly slower of what we measured in mice (Fig. 3C and D), but faster than what is known in rats[37].

We also tested the sensitivity of isolated hearts to positive and negative modulation with natural agonists of β-adrenergic and vagal modulation. When the β-adrenergic agonist epinephrine (30 nM) was perfused in the Langendorff system or on the atrial preparations analysed by optical mapping, we observed only a tendency to positive chronotropic modulation (Fig. 3A and F). Conversely, the vagal effector acetylcholine (50 nM) caused a significant rate reduction (Fig. 3A and F). For both adrenergic and vagal effectors, in the atrial preparation, the modulations of SAN rate was associated with delocalization of the leading regions respectively toward the frontal or caudal portion of the SAN (Fig. 3E), similarly to what we previously demonstrated in mice[41]. We further tested the β-adrenergic response with saturating doses[42] of the agonist isoprenaline (1 µM) and again we found only a non-significant tendency to AP rate increase that could be related to the advanced age of the animals used (Suppl. Fig.3). Conversely, when we directly activated the L-type Ca^{2+} channels with the agonist BayK8644 (1 µM) in atrial preparation previously exposed to β-adrenergic stimulation with epinephrine or isoprenaline, we found a significant increase of AP rate. This significant change of AP rate was indicative of the ability of L-type Ca^{2+} channels to increase pacemaker rate despite the impairment of the β-adrenergic pathway.

3. Native pacemaker myocytes isolated from the mouse lemur SAN conduct the ionic currents I_f and I_{Ca}, and generate spontaneous APs and intracellular Ca^{2+} transients.

To characterize the fundamental mechanism of SAN pacemaker activity at the cellular level, we freshly isolated single pacemaker myocytes from the SAN tissue of the mouse lemur. After enzymatic digestion, we observed single pacemaker myocytes with self-contractile properties (data not shown) and spindle shapes similar to SAN pacemaker myocytes of mice[3], rats[43] and humans[21] (Fig. 4A).

Immunostaining of single pacemaker myocytes and intact mouse lemur SAN tissues revealed the expression of HCN4 channels, which are important marker of pacemaker activity (Fig. 4B, C and D). In

the pacemaker myocytes isolated from the SAN we attempted to record three of the main currents involved in the mechanism of automaticity: I_f, and the L-type and T-type Ca^{2+} currents, $I_{Ca,L}$ and $I_{Ca,T}$, respectively (Fig. 5A and B). In addition, we recorded the inward-rectifier K^+ current I_{K1} (Fig. 5A and B), which has been reported also in the SAN of mice[44] and rats[43].

When cell capacitance was considered, the current densities of I_{K1} and I_f were similar to that recorded in rat SAN myocytes[43]. Current density of I_f also appeared very similar to that in mice[45], i.e. about 2.5 higher than in humans[21]. In comparison to mouse, SAN myocytes from *M. murinus*, showed reduced total Ca^{2+} current ($I_{Ca,Tot}$: $I_{Ca,L}$ + $I_{Ca,T}$), possibly due to lower $I_{Ca,T}$. However, the density of $I_{Ca,L}$ appeared similar to that in SAN myocytes from mice[46], with a similar threshold of activation, but with a peak of current density at 0 mV, which is more positive that the peak of current in mice but similar to what has been shown in rats[43].

Next we superfused the lemur SAN myocytes with Tyrode's control solution, and performed patch-clamp recordings of pacemaker activity. On average we recorded 148 ± 22 APs/min (n=7; Fig. 6A). Moreover, under the same control condition in these myocytes we recorded spontaneous generation of intracellular Ca^{2+} transients at a rate of 82 ± 23 per min (n=11 Fig. 6B).

We then sought to modulate the pacemaker activity of *M. murinus* SAN myocytes with the natural agonists of the β-adrenergic and muscarinic receptors, epinephrine and acetylcholine (Fig. 6B). Analysing SAN cells recorded by patch-clamp or line scan, we found only a tendency to rate increase after epinephrine stimulation (Fig. 6B and C), in accordance to what we found with the intact cardiac tissues. Conversely, acetylcholine superfusion in the same type of SAN myocytes, significantly reduced the rate of APs and intracellular Ca^{2+} transients (Fig. 6B and C), replicating what we found the intact cardiac tissues. In addition, the specific I_f blocker ivabradine (1 µM) significantly decreased the rate of intracellular Ca^{2+} transients, while the blocker of ryanodine receptor (RyR), ryanodine (Ry) cause a strong tendency to decrease the rate of intracellular Ca^{2+} transients (Fig. 6B and D).

4. Analysis of automaticity in PML cells differentiated from muscle-derived stem cells (MDSC).

Although small primates like *M. murinus* are easier to keep in captivity, their availability remains limited and they will be always less available than classical rodent models, like mice and rats. On the other hand, *in vitro* preparations of stem cells are increasingly used to understand cell physiology and the function of ion channels[47]. Therefore, to have an *in vitro* system to easily test pharmacological approaches in cardiac cells from primates, we used skeletal muscle biopsies of *M. murinus* and we attempted to differentiate cells that replicate some of the characteristics of native SAN pacemaker myocytes. Initially, skeletal muscle-derived stem cells (MDSCs) consisted of heterogeneous pluripotent stem cells. Taking advantage of the pre-plating technique to isolate these cells[34], we were able to isolate a subpopulation of cells that present some of the typical features of native SAN pacemaker myocytes, as we have done in mice[35]. For that, we cultured MDSCs *in vitro* for 66 to 74 days, to ensure a full differentiation towards the sustained beating phenotype of pacemaker-like (PML) cells[35].

Similar to the phenotype of SAN pacemaker myocytes, PML cells expressed HCN4 and L-type $Ca_v1.3$ channels as well as Connexin 45 (Fig. 7A), which are all typical markers of native SAN pacemaker myocytes in mice[3]. Moreover, like native pacemaker myocytes isolated from the *M. murinus* SAN, PML cells showed spontaneous contractions that could be measured by the coordinated movement of their edges. This allowed us to record the rate of the spontaneous activity in these cultured cells with no need for enzymatic digestion or reagent incubation. Our PML cells were thus in an amenable physiological condition for modulator compound dose-response analysis.

We therefore measured the spontaneous contraction rate in PML cells under control conditions and after superfusion with increasing doses of epinephrine, acetylcholine, ivabradine and I_{Kr} inhibitor E4031. Under control conditions, PML cells showed spontaneous contractility at a rate of 171 ± 13 cell beats/min (n=33; Fig. 7B), a rate comparable to AP firing measured in native pacemaker myocytes of mouse lemur (see above). After exposure to modulator compounds in the extracellular medium, PML cells responded accordingly with the expression of functional HCN4 f-channels, I_{Kr} and membrane

receptors typical of native pacemaker myocytes, with a significant and reproducible acceleration or deceleration that was proportional to the concentration of the drug tested (Fig 7B and C). Indeed, both the I_f current blocker ivabradine and the I_{Kr} inhibitor E-4031 decreased the rate of spontaneous contractions of PML cells, in agreement with functional expression of HCN4 and ERG channels.

PML cells revealed the ability to generate spontaneous APs, with a rate of 161 ± 14 APs/min (n=12; Fig. 7D), which again is comparable with what we recorded in native cardiac pacemaker myocytes of *M. murinus* (see above). The larger availability of cells prepared *in vitro*, in comparison with native SAN myocytes, allowed for a wider pharmacological screening of drugs known to modulate cardiac pacemaker activity at the cellular level. Indeed, we tested β-adrenergic and muscarinic modulation by superfusing the natural agonists epinephrine and acetylcholine. In addition, we tested the functional presence of cardiac sodium channels by superfusing the specific blocker tetrodotoxin.

The firing rate of PML cells nearly doubled the number of APs/min by 87 ± 25% under β-adrenergic stimulation with epinephrine (30nM), while acetylcholine (50 nm) and tetrodotoxin nearly halved the spontaneous rate of PML cells, reducing them by 49 ± 11% and 41 ± 13%, respectively (Fig 7D and E).

Discussion

The mouse lemur, *Microcebus murinus,* is an arboreal and nocturnal primate, among the smallest and more ancestral of the primate order[48]. This lemur is an emerging model to study neurodegenerative diseases related to ageing because it better replicate the corresponding neurophysiology of human. Given the importance of the heart-brain crosstalk in modulating heart rate[49] and the genetic proximity of mouse lemurs to humans this lemur could also help study cardiac physiology[48]. In addition, its small size and facile reproduction make it affordable to breed in captivity, maintaining a viable population that might help to preserve this species for future reintroduction into the wild to fight against habitat loss.

Impaired modulation of the heart by the autonomic nervous system has been related to ageing. Importantly like humans the mouse lemur present spontaneous neurodegeneration with ageing, a feature that is not found in mice[25]. This degeneration likely affects the regulation of the cardiovascular system function by the autonomic nervous system. Thus *M. murinus* could better recapitulate a neural environment similar to humans, to study cardiac pacemaker activity and age-related dysfunctions of the sinoatrial node.

Despite these advantages, so far, there are no studies that investigated the cardiac physiology of *M. murinus*. To approach the cardiac physiology of these lemurs, we applied a range of techniques that allowed us to characterize heart rate and pacemaker activity of *M. murinus* and compare those with previous data published in rodents of similar size (mice and rats), or in humans.

These comparisons showed that the frequency of heartbeat in *M. murinus* overlaps the average heart rate in mice and rats[37 40], which is consistent with the small size of this primate. On the other hand, *M. murinus* presents cardiac features that distinguish these animals from small rodents. In particular, the electrocardiograms of mouse lemurs present T waves clearly separated from the QRS complex, which suggests a dynamic of repolarization more similar to large mamals[38] and humans[36 39]. In addition, we observed recurrent decreases of heartbeat down to 200 or less bpm, that were often followed by sudden heart rate increase. Physiological heart rate decrease at rest, determined by intracellular release of acetylcholine in SAN pacemaker myocytes is a fast phenomenon that generally cause oscillation of heart rate for few seconds[5]. The longer dynamic of the heart rate decrease observed in mouse lemurs suggests that this is a different phenomenon. We do not have an immediate explanation for this heart rate variations, but its prolonged dynamic suggests that it could be a physiological phenomenon with more complex causes than the classical vagal modulation[5]. We hypothesize that this slow heart rate decrease could be related to the mechanism that allows *M. murinus* to enter into a torpor state, to save energy when the outside temperature drops[29 30].

Our analysis of atrial preparations in *M. murinus* revealed that these portion of the heart is about twice those of mice. In accordance with a bigger size, the APs frequency of the intact SAN tissue in *M. murinus* was significantly slower than the equivalent preparation in mice. Moreover, in mouse lemurs' atrial preparations we observed larger left versus right atria. This difference could be consequent to the old age of the mouse lemurs used for these experiments and could constitute a further point of similarity with human cardiac physiology. Indeed, in patients it is known that left atria are enlarged with ageing to compensate for the deficiency of left ventricle contraction to ensure correct blood circulation[50]. The same compensation might take place in mouse lemurs.

Studying single pacemaker myocytes isolated from the mouse lemur SAN we revealed the expression of HCN4 channels as well as the conduction of I_f. Also, we observed that the automaticity of these

pacemaker myocytes was negatively regulated by the I_f blocker Ivabradine and by ryanodine, which locks the intracellular Ca^{2+} release from the sarcoplasmic reticulum.

The slowing of pacemaker activity by I_f blockers and ryanodine has been consistently observed in SAN myocytes from all mammalian models used so far and is integrated in currently accepted models of pacemaker activity[51,52]. In addition, in single mouse lemur pacemaker myocytes we demonstrated the conduction of $I_{Ca,T}$ and the low threshold activated $I_{Ca,L}$. The recording of these currents, as well as the pharmacological responses to the $I_{Ca,L}$ agonist BayK8644 suggest that depolarization in pacemaker myocytes of *M. murinus* appends with a membrane mechanism similar to what is known for mice[3 2 46]. Thus, we hypothesize that the same mechanism could be extended to human, given the common genetic origin with mouse lemurs.

Similarly to what was previously reported in SAN myocytes from mice[44] and rats[43], in mouse lemurs we recorded Ba^{2+} sensitive I_{K1} at densities comparable to that observed in rat SAN myocytes[43]. This current is almost absent in SAN myocytes of larger mammals, while it is conducted at a higher density in the working myocardium and in Purkinje fibres, where it is responsible for negative diastolic potential versus SAN myocytes[3]. Thus, the presence of this current in mouse lemurs could indicate a specificity of small mammals that could represent a limitation in the extrapolation of cardiac results to humans.

Concerning the autonomic modulation of the heart by the autonomic nervous system, we found that β-adrenergic stimulation with epinephrine of single cells, SAN tissue or whole heart, only tended to increase heart rate. Conversely, further stimulation with the $I_{Ca,L}$ agonist BayK8644 significantly increase AP rate suggesting that the sympathetic pathways could be impaired by the old age of the lemurs used, but that their SAN is still able to increase pacemaker rate. On the other hand, muscarinic modulation by acetylcholine superfusion significantly reduced the rate of pacemaking.

Finally, we obtained MDSCs from skeletal muscle biopsies of mouse lemurs. We cultured these cells using a technique that we have been previously applied in mice to differentiate PML cells that share similar features with native SAN pacemaker myocytes[34,35]. In our recordings, these PML cells contracted spontaneously and generated APs at a rate comparable to native mouse lemur pacemaker myocytes. Moreover, PML cells expressed the classical markers of native pacemaker myocytes, notably HCN4, $Ca_v1.3$ and Cx 45, and respondedto positive and negative β-adrenergic and muscarinic chronotropic stimulation.

A further investigation is ongoing to better understand the degree of similarity between PML cells and native SAN myocytes[35]. Nevertheless, our results indicate that the degree of similarity between native pacemaker myocytes and PML cells could make these cells a valid model for preliminary investigation of pharmacological effects on the mechanism of cardiac pacemaking in primates.

In conclusion, we provide the first characterization of the cardiac pacemaker activity of mouse lemurs and we propose this primate as a new model to investigate cardiac dysfunctions related to ageing in a neurodegenerative context similar to humans. In the light of the close genetic origin, mouse lemurs opens the way to an easier translation of cardiac results from animal models to human physiology. Moreover, this initial characterization will help the future understanding of the mechanism behind the torpor state of mouse lemurs. Although the ability to enter torpor could appear anecdotal at first, it could have important applications in inducing artificial comas, avoiding organ failure, and for the slowdown of human metabolism during long-term space flight[30].

Methods

1. Care and use of animals.

This investigation conformed to the Guide for the Care and Use of Laboratory Animals published by the US national Institute of Health (NIH Publication No. 85–23, revised 1996) and European directives (2010/63/EU). Male and female *M. murinus*, of 1 to 11 years of age, were used. Specifically, animals from 1 to 5 years were used for telemetry recording with minimally invasive or external electrocardiogram devices that allowed reintegration of the animals to the colony after the experimentation. Conversely, animals from 6 to 11 years, that after natural ageing must be euthanized for factors hampering normal life, like weight loss, were used for all the other experiments. This approach reduces the need of animals in the respect of the "three R's" of animal welfare: replacement, reduction, and refinement.

Mouse lemurs used for implantation and electrocardiogram recordings were hosted at the mouse lemur colony of Brunoy (MECADEV, MNHN/CNRS, IBISA Platform, agreement F 91.114.1, DDPP, Essonne, France) under the approval of the Cuvier Ethical Committee (Committee number 68 of the "Comité National de Réflexion Ethique sur l'Expérimentation Animale"), under authorization number 68-018. In the respect of the principle of "three R's" of animal welfare, the use of these data, collected during another project for other purpose, allowed reduction of animal use since we did not have to implant new animals for the present project. All the other mouse lemurs came from the colony housed at RAM-CECEMA (license approval 34-05-026-FS, DDPP, Hérault, France). Their use was conducted under the approval of the CEEA-LR Ethical Committee (Committee number 36). Animals were euthanized at the end of their lives and all organs were collected immediately for biomedical research.

2. Housing conditions

All animals were housed in cages equipped with wood branches for climbing activities as well as wooden sleeping boxes mimicking the natural sleeping sites of mouse lemurs. The temperature and the humidity of the rooms were maintained at 25–27 °C and at 55–65%, respectively. In captivity, the artificial daily light-dark cycles within the housing rooms are changed to mimic season alternation, with periods of 6 months of summer-like long days (14 h of light and 10 h of darkness, denoted 14:10) and 6 months of winter-like short days (10 h of light and 14 h of darkness, denoted 10:14). Animals were fed ad libitum with fresh fruit, worms and a homemade mixture as in ref[53].

3. Electrocardiogram recordings.

One-lead electrocardiograms were recorded from freely moving and anaesthetized mouse lemurs. For electrocardiogram recordings in freely moving animals implanted with a transmitter, surgery was conducted in sterile conditions, under veterinarian supervision. After administration of diazepam (Valium, 1 mg/100 *g*, i.m.) and buprenorphine (0.005 mg/100 *g*, i.m.), anaesthesia was induced and maintained by 1–3% isoflurane inhalation. Body temperature was maintained with a heating pad, and the animal's eyes were protected with ocular gel (Ocry−gel; Laboratoire TVM, Lempdes, France). A small transmitter (PhysioTel F20-EET, 3.9 *g*, 1.9 cc; Data Sciences International TM, DSI, St. Paul, United States) connected with 1 pair of electrode wires (silicon elastomer insulated stainless-steel wires, diameter: 0.3 mm) was inserted inside the peritoneal cavity of the animal. Electrode wires were led subcutaneously from the abdomen to the thorax muscle and were sutured using non-absorbable polyamide monofilament suture thread, similarly to the procedure described in mice[40]. After surgery, nociception was minimized by subcutaneous injection of analgesic and anti-inflammatory drugs (meloxicam, 0.2 mg/100 *g*). electrocardiogram signals were recorded using a telemetry receiver and

an analog-to-digital conversion data acquisition system (Data Sciences International TM, DSI, St. Paul, United States). Heart rate and heart rate variability data were analyzed with the dedicated softwares Labchart 8 (ADInstruments, Dunedin, New Zealand) and ecgAUTO v3.3.5.12 (emka TECHNOLOGIES, Paris, France).

For external electrocardiograms, we used gel electrodes (Youpin Hipee disposable electrocardiogram electrode patch) and the Xiaomi Youpin HiPee Intelligent Dynamic Holter produced by Zhejiang Helowin Medical Technology Co., Ltd (Hangzhou, China), to obtain one lead recording of heart rate. Soft surgical tape helps to keep the Holter on the back of mouse lemurs. Before that, the animals were shaved in the contact points with the gel electrodes, to facilitate the conduction of the signal through the skin. Electrocardiogram recordings were obtained through dedicated application software provided by the Helowin company and analyzed with the dedicated softwares Labchart 8 (ADInstruments, Dunedin, New Zealand). 5 min of electrocardiogram recordings obtained in the first 15 min after the application of the Holter were used to obtain heart rate during animal handling.

For ELECTROCARDIOGRAM recordings under anaesthesia, we constantly exposed mouse lemurs to 1.5% isofluorane. Body temperature of mouse lemurs was continuously maintained at 36° - 37°C using a heated pad connected to a controller that received feedback from a temperature sensor attached to the animal. Ag/AgCl gel-coated electrocardiogram electrodes (Unomedical; Herlev, Danimarca) were attached to the superior right and to the two inferior limbs of the mouse lemurs. The electrodes were connected to a standard one-lead electrocardiogram amplifier module (EMKA Technologies, Paris, France), which included high- and low-pass filters (set to 0.05 Hz and 500 Hz, respectively) and a gain selection device (set to 1,000-fold). Signals were digitized continuously at 2 kHz and recorded using an IOX data acquisition system (emka TECHNOLOGIES, Paris, France). The recordings were carried out for a 45-minute period, and the software ECGAuto (emka TECHNOLOGIES, Paris, France) was used to perform offline analysis of the recorded data. For each mouse lemur the mean HR, its standard deviation and the parameters characterizing the electrocardiogram wave, were calculated at 30-min intervals starting 10 min after the beginning of each 45-min recording.

4. Langendorff perfused hearts.

After general anaesthesia, consisting of 0.1 mg/g of ketamine (Imalgène, Merial, Bourgelat France) and complete loss of hind-limb reflex, indicative of cerebral death, we removed the heart from the thoracic cage of mouse lemurs and quickly mounted it on a Langendorff apparatus (Isolated heart system; emka TECHNOLOGIES, Paris, France) at a constant pressure of 80 mm Hg with normal Tyrode's solution. Perfused hearts were immersed in the water-jacked bath and maintained at 36°C. electrocardiograms were continuously recorded by Ag-AgCl electrodes positioned on the epicardial side of the right atrium close to the SAN and near the apex. Heart rate was allowed to stabilize for at least 30 min before perfusion of 30 nM epinephrine or 50 nM acetylcholine.

5. Atrial preparation and optical voltage mapping.

Atrial preparations (including the SAN, right and left atria) were obtained as described previously[42]. Briefly, as described in the previous paragraph, after general anaesthesia with ketamine and complete loss of hind-limb reflex, we removed the heart from the thoracic cage of the animal. Then, we cut the coronary sinus and, starting from it, we removed the ventricles from the heart. We used a stereomicroscope (SZX16, Olympus; Tokyo, Japan) with low magnification (7X) to trans-illuminate and directly visualize the remaining atrial preparation constituted by the SAN plus right and left atria. We identified the SAN region using the borders of the superior and inferior vena cava, the crista terminalis and the interatrial septum as landmarks[23]. The atrial preparation was pinned to the bottom of an

optical chamber (Fluorodish, FD35PDL-100, WPI; Sarasota, FL) coated with ~2 mm of clear Sylgard (Sylgard 184 Silicone elastomer kit; Dow Corning; Midland, MI). To avoid interference from secondary pacemaker tissues we removed the atrioventricular node from the preparation.

For comparative experiments, 24 month-old mice were used to match the old age of *M. murinus* (from 6 to 11 years old) used to obtain tissue preparation of the SAN. As for *M. murinus* the investigation with mice conforms to the European directives (2010/63/EU) for the Care and Use of Laboratory Animals and was approved by the French Ministry of Agriculture (N° D34-172-13). Briefly, mice were anaesthetized with 0.01 mg/g xylazine (Rompun 2%, Bayer AG, Leverkusen Germany), 0.1 mg/g ketamine (Imalgène, Merial, Bourgelat France) and 0.2 mg/g Na-Pentobarbital (CEVA, France). Then, after complete loss of hind-limb reflex, we removed the heart from the thoracic cage of the animal and we dissected it to obtain the entire atrial preparation [42]

To analyse voltage changes in the atrial preparation we loaded it by immersing the tissue in a Tyrode's solution containing the voltage-sensitive indicator Di-4-ANEPPS (2 µmol/L; AAT Bioquest, Sunnyvale, California). This immersion was performed at room temperature (20-22°C) and lasted for at least 30 min. To maintain proper oxygenation, the chamber containing the tissue was maintained under agitation for the whole loading period. After the loading step, the tissue was washed in dye-free Tyrode for 15 min. During this step, the temperature was slowly increased to 34-36° C. The atrial preparation was then constantly superfused at 34-36° C and imaged by high-speed optical voltage mapping (1000 to 333 frames/s) on a MiCAM03 Camera - 256x256 pixel CMOS sensor, 17.6x17.6 mm (SciMedia; Costa Mesa, CA). This camera was mounted on a THT microscope, with two objectives (2X and 1.6X) that generated a field of view of 22 x 22 mm. A system constituted by a 150 W halogen light and a built-in shutter (SciMedia; Costa Mesa, California) was used as the excitation source of light for the voltage dye. The filter set included a 531/50 nm excitation filter, 580 nm dichroic mirror, and 580 long-pass emission filter. To avoid motion artefacts, we blocked mechanical activity using blebbistatin (10 µM; Tocris Bioscience; Bristol, UK)[42]. Optical raw data were analysed using dedicated software from the camera developer, BV workbench (Brainvision; Tokyo, Japan), in combination with ClampFit (ver. 10.0.7, Molecular Devices, LLC; San Jose, California).

6. Isolation of SAN myocytes.

The SAN tissue of mouse lemur was isolated as described above and cut in tissue strips. Strips were then transferred into a low-Ca^{2+}, low-Mg^{2+} solution containing (in mM): 140.0 NaCl, 5.4 KCl, 0.5 $MgCl_2$, 0.2 $CaCl_2$, 1.2 KH_2PO_4, 50.0 taurine, 5.5 d-glucose and 1.0 mg/ml BSA, plus 5.0 mM HEPES-NaOH (adjusted to pH 6.9 with NaOH). The tissue was enzymatically digested by adding 229 U/ml collagenase type II (Worthington Biochemical Corporation), 1.9 U/ml elastase (Boehringer Mannheim), 0.9 U/ml protease (Sigma-Aldrich), 1 mg/ml BSA, and 200 µM $CaCl_2$. Tissue digestion was performed for a variable time of 9–13 min at 35°C with manual agitation using a flame-forged Pasteur pipette. Tissue strips were then washed and transferred into a medium containing (in mM): 70.0 L-glutamic acid, 20.0 KCl, 80.0 KOH, 10.0 (±) D-β-OH-butyric acid, 10.0 KH_2PO_4, 10.0 taurine, 1 mg/ml BSA, and 10.0 HEPES-KOH, adjusted at pH 7.4 with KOH. SAN myocytes were manually dissociated in KB solution at 35°C for about 10 min. Cellular automaticity was recovered by readapting the myocytes to physiological extracellular Na^+ and Ca^{2+} concentrations by adding first a solutions containing (in mM): 10.0 NaCl, 1.8 $CaCl_2$, and, subsequently and then normal Tyrode's solution containing 1 mg/ml BSA. The final storage solution contained (in mM): 100.0 NaCl, 35.0 KCl, 1.3 $CaCl_2$, 0.7 $MgCl_2$, 14.0 l-glutamic acid, 2.0 (±)D- β -OH-butyric acid, 2.0 KH_2PO_4, 2.0 taurine, and 1.0 mg/ml BSA, pH 7.4. Cells were then stored at room temperature until use. All chemicals were obtained from Sigma-Aldrich, except for the (±)D- β - OHbutyric acid, which was purchased from Fluka Chemika. For electrophysiological recording, SAN

myocytes in the storage solution were harvested in special custom-made recording Plexiglas chambers.

7. Preparing and culturing of MDSCs and PML cells.

MDSCs were prepared using the modified preplate procedure originally described by Arsic et al.[34] and modified recently in the reference[35]. Briefly, after general anaesthesia, consisting of 0.1 mg/g of ketamine (Imalgène, Merial, Bourgelat France) and complete loss of hind-limb reflex indicative of cerebral death, the hind limb muscles of mouse lemurs were removed, minced and enzymatically dissociated at 37°C for 45 min in 0.2% collagenase A (Roche) and 1 mg/ml dispase (GibcoBRL). After digestion, muscle cells were passed through a 40 µm nylon cell strainer (BD Falcon) and centrifuged at 328 g for 10 min. Pelleted cells were washed twice in phosphate buffer saline (PBS), suspended in the growth medium [DMEM/F12 (Sigma), 16% fetal bovine serum (PAA), 1% Ultroser G (Pall Life Sciences), antibiotic-antimycotic mix (Gibco)] and plated on uncoated dishes (NUNC). After an initial 40 min pre-plating, non-adherent pluripotent stem cells were transferred to a new dish every 24 h for 4 to 6 days. For confocal microscopy experiments, cells were seeded onto glass-bottom chambers (Fluorodish, FD35PDL-100, WPI; Sarasota, FL). Otherwise, they were cultured in standard 35 mm petri dishes. To ensure a full maturation of spontaneously differentiated stem cells, culturing was prolonged for 1 to 3 months before experimentation, and PML cells were selected as spontaneously-contractile cells, based on their morphology.

8. Patch-clamp recordings of *M. murinus* SAN myocytes and PML cells.

Myocytes isolated from the *M. murinus* SANs were prepared as described in the previous sections, while PML cells were enzymatically treated with brief digestions, of 3 to 5 minutes, at 37 °C with 229 U/ml collagenase type II (Worthington Biochemical Corporation), and washed in Tyrode solution for enzyme removal, leaving cells in their culture petri-dish. The basal extracellular Tyrode's solution used in all recordings contained (in mM): 140.0 NaCl, 5.4 KCl, 1.8 CaCl2, 1.0 MgC_{l2}, 5.0 HEPES-NaOH, 5.5 and d-glucose (adjusted to pH 7.4 with NaOH). To measure the hyperpolarization-activated current I_f, we employed standard Tyrode's solution in the presence or absence of 2 mM Ba^{2+} to block the inward rectifier K^+ current I_{K1}, without affecting I_f[54]. I_{K1} was subtracted from I_f as the net Ba^{2+}-sensitive conductance, while I_f was extracted as the currents not blocked under perfusion of Ba^{2+}, but subsequently inhibited in the presence of 5 mM Cs^+. $I_{Ca,L}$ and $I_{Ca,T}$ were recorded as previously described[46]. In particular, I_{CaToT} (I_{CaT} + I_{CaL}) was recorded from a holding potential of −80 mV in isolated SAN myocytes. Then after switching HP to −55 mV we inactivated I_{CaT} to obtain only $I_{Ca,L}$.

AP firing activity was measured in the current clamp (CC) configuration. Patch-clamp electrodes had a resistance of 4–5 MΩ when filled with an intracellular solution containing (in mM): 130.0 K^+-aspartate; 10.0 NaCl; 2.0 ATP-Na^+ salt, 6.6 creatine phosphate, 0.1 GTP-Mg^{2+}, 0.04 $CaCl_2$ (pCa = 7.0), and 10.0 Hepes KOH (adjusted to pH 7.2 with KOH). For the modulation of AP firing, we perfused 30 nM epinephrine, 50 nM acetylcholine or 30 µM tetrodotoxin. Compounds were added to the external medium and perfused through a pipette at a controlled temperature of 36°C. Pacemaker activity of SANs and PML cells were recorded under perforated patch conditions by adding 50 µM β-escin to the pipette solution.

9. Confocal imaging of intracellular Ca^{2+} fluctuations.

Intracellular Ca^{2+} release was recorded in SAN pacemaker myocytes loaded with Fluo-4 AM at room temperature (22-24°C). Pacemaker myocytes were distinguished from other excitable myocyte types (i.e. atrial myocytes) by their morphology (spindle, spider and elongated) and size (~ 10 µm diameter). Images were obtained by confocal microscopy (Meta Zeiss LSM 510 and Zeiss LSM 780), by scanning

the myocyte with an argon laser in line scan configuration (1.54 ms line rate); fluorescence was excited at 488 nm and emissions were collected at >505 nm. A 63x oil immersion objective was used to record Ca^{2+} release in isolated pacemaker myocytes. Images were corrected for the background fluorescence and the fluorescence values (F) were normalized to the basal fluorescence (F0) to obtain the fluorescence ratio (F/F0). Integrals of light intensity were analysed by pClamp software (ver.9, Molecular Devices) and spontaneous Ca^{2+} transients were analysed by ImageJ software.

10. Measuring PML cell shortening.

PML cell were placed on the stage of an inverted microscope (Olympus IX71). Cell contractions were recorded using a video-based edge-detection system (IonOptix™). Digitized images were collected at 120 Hz using an IonOptix™ Myocam-S CCD camera, and displayed within the IonWizard™ acquisition software (IonOptix™). To measure changes in cells length, two cursors were placed at opposite edges of the cell samples, where the difference in optical density (maximum: dark; minimum: light) generated the higher contrast. Cell shortening was then assessed by the simultaneous movement of the cursors. For the modulation of contraction rate, we perfused epinephrine (1 nM to 1 µM), acetylcholine (1 to 50 nM), ivabradine (3 nM to 3 µM) and E4031 (300 nM and 3 µM). Compounds were added to the external medium and perfused through a pipette at a controlled temperature of 36°C.

11. Immunofluorescence analysis

Immunofluorescence analysis was performed on SAN tissue, native SAN pacemaker myocytes and PML cells, as in ref [34]. Tissues and cells were fixed with 3.7% formaldehyde for 30 and 5 min, respectively. Then these samples were permeabilized for 30 s in -20°C acetone, preincubated for 30 min with 0.5% BSA in PBS. Cells were then incubated for 1h at 37°C with primary antibodies against HCN4, (1:100, Alomone), sarcomeric alpha-actinin, clone EA-53 (1:100, Sigma-Aldrich), connexin 45 (1:100, H-85, Santa Cruz Biotechnology), $Ca_v1.3$ Ca^{2+} channel polyclonal antibody (N38.8, neuromab UC Davis), cardiac troponin I (1:100, Millipore), caveolin 3 (1:100, BD Transduction Laboratories) or myogenin (1:50, sc576 santa cruz). Specific staining was revealed using anti-mouse or anti-rabbit Alexa Fluor 488 and Alexa Fluor 555-conjugated secondary antibodies (InVitrogen) with Hoechst33358 nuclear stain (0,1 µg/ml) for 30 min at 37°C.

12. Statistical analysis

Significance was evaluated through Student's T test or one-way- or two-way ANOVA as specified in figure legends. When testing statistical differences, results were considered significant with $p<0.05$. Data analysis were performed with GraphPad Prism 9.0.

Acknowledgments

We are thankful to the personnel of the animal facility of the lemur colony at Brunoy, to the animal facility at RAM-CECEMA, the MRI platform of imaging and the statistic platform Statabio. We thank Fu Lingjian, Dr. Yuquan Wang and Emma Zub for helping with software installation and explanation. M-L DiFrancesco was recipient of a postdoctoral fellowship by the Laboratory of Excellence *Ion Channel Science and Therapeutics* supported by a grant from *Agence Nationale de la Recherche* (ANR-11-LABX-0015). This work was supported by ANR grants (2010-BLAN-1128-01 and ANR-15-

CE14-0004-01 to M.E.M.) and the *Fondation Leducq* (TNE FANTASY 19CVD03 to Matteo E. Mangoni and Peter J. Mohler).

Figures:

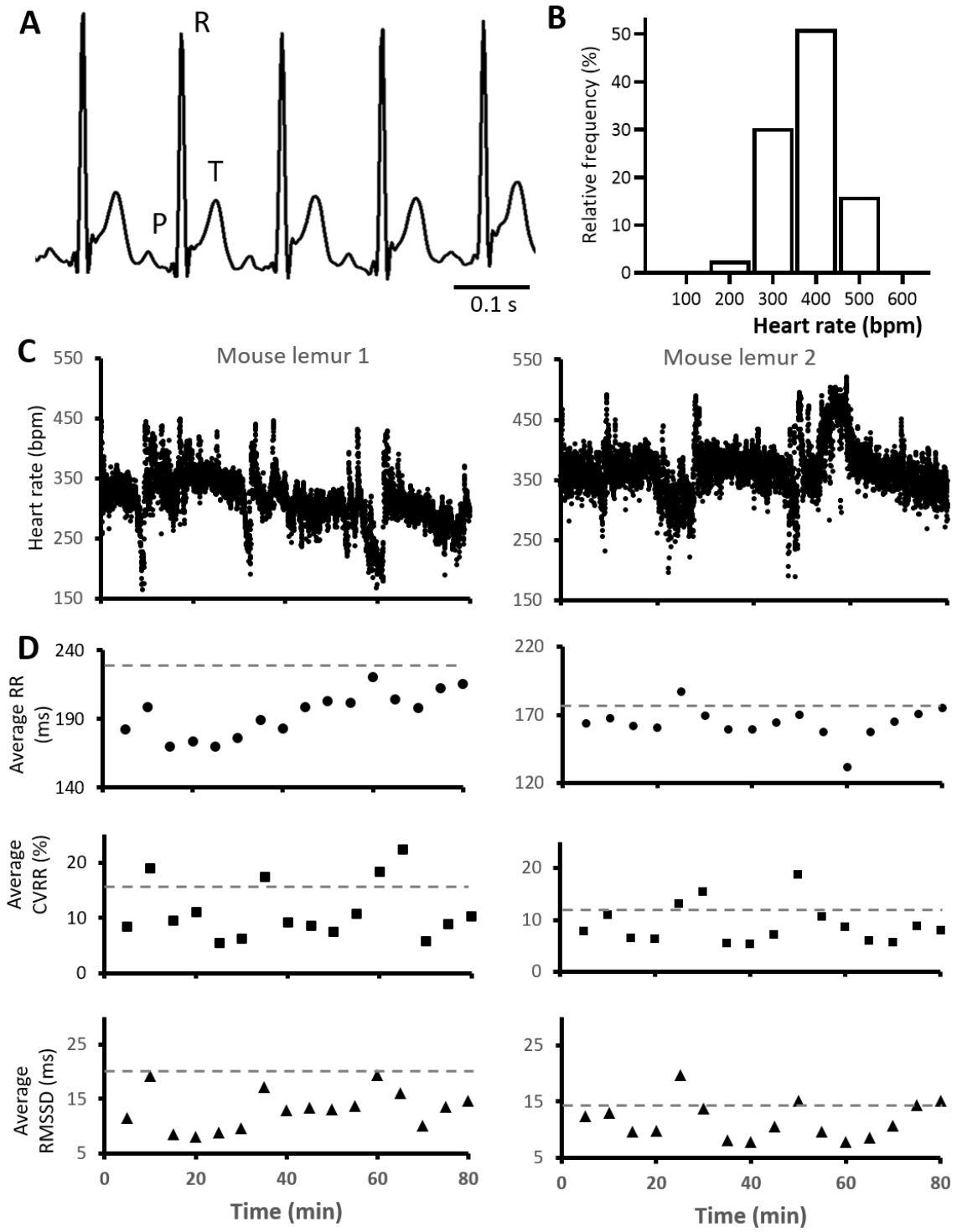

Figure 1: *In vivo* recording of cardiac activity in mouse lemurs.

A: Example traces of electrocardiograms in freely moving *M. murinus*. Note P, R and T waves. **B:** Range of heart rate measured during 22 hours of electrocardiogram recording in one animal. **C:** Example of 80 min recording in two mouse lemurs showing heart rate changes versus time. Note the cyclical decrease of heart rate to very low frequencies. **D:** Plots obtained by averaging every 5 min, the interval

between successive heart beats (RR interval), its coefficient of variability (CVRR) and the root mean square of successive differences between heart beats (RMSSD), for the recordings shown in C. Dashed gray lines indicate the threshold of mean + SD for each of the parameters reported.

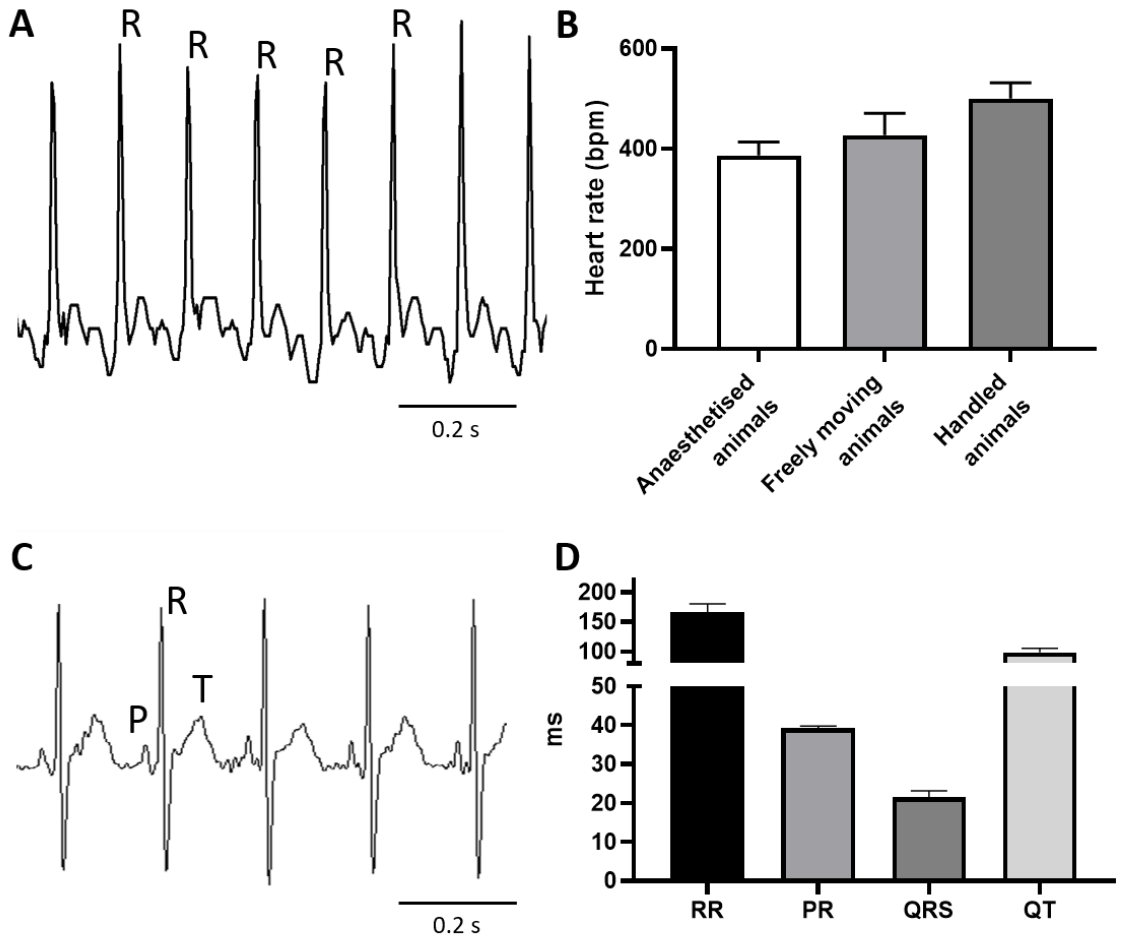

Figure 2: Cardiac activity of mouse lemurs during handling or anaesthesia.

A: Example trace of electrocardiograms from mouse lemurs recorded with an external device during experimental handling. **B:** Comparison of heart rate in anaesthetized, freely moving and handled mouse lemurs (n=5, n=4, n=3 respectively). **C:** Electrocardiograms from anaesthetized mouse lemurs. Note P, R and T waves. **D:** interval between successive heart beats (RR), interval between atrial and ventricular contraction (PR), length of the ventricular depolarization (QRS) and interval between ventricular depolarization and repolarization (QT) characterizing the electrocardiogram waveform of anaesthetized mouse lemurs (n=5).

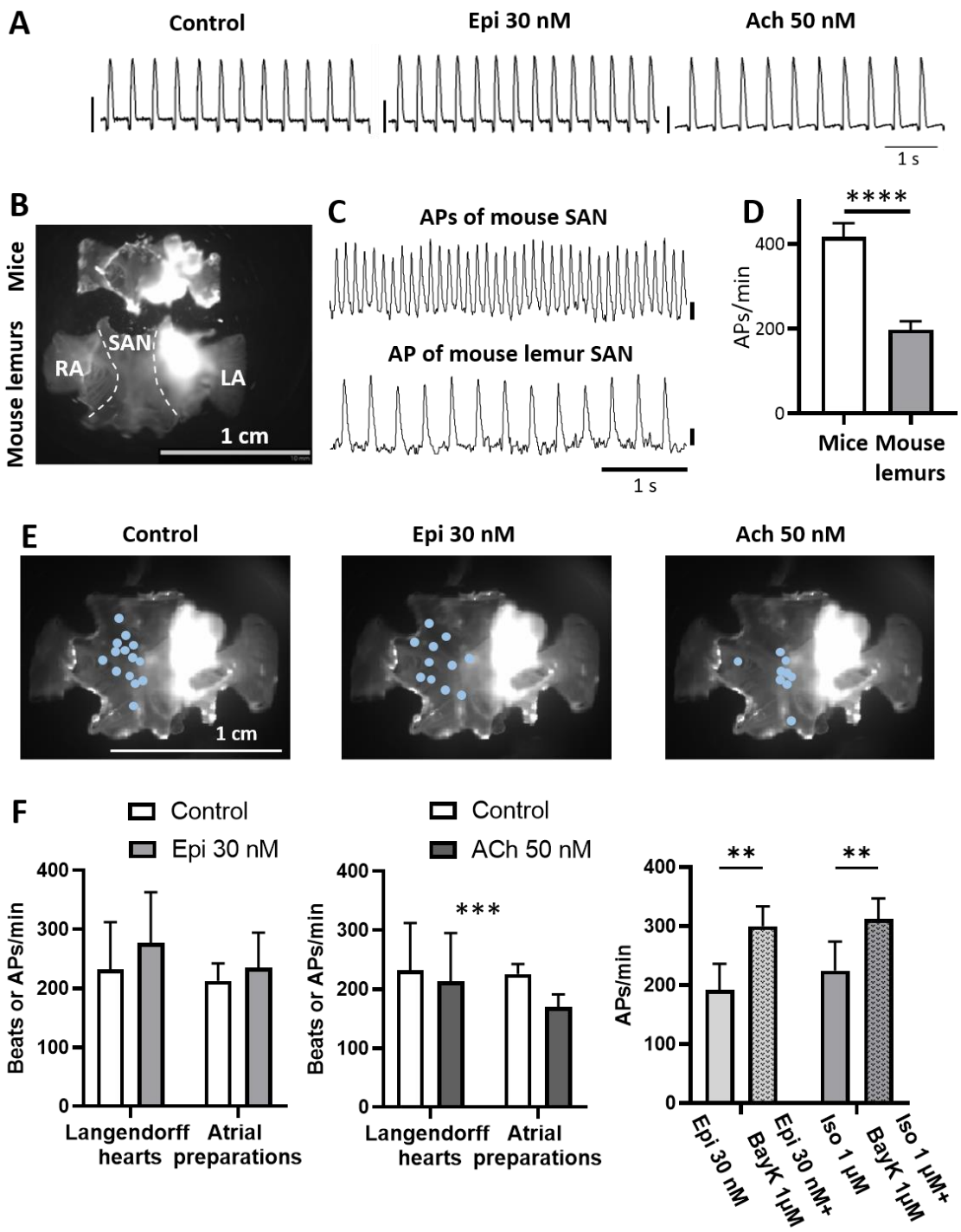

Figure 3: Pacemaker activity of isolated hearts and atrial preparations. A: Example traces of electrical activity from isolated mouse lemur hearts maintained alive through constant perfusion with a Langendorff system. Traces have been recorded under control and perfusion of epinephrine (Epi; 30 nM) and acetylcholine (ACh 50 nM). Scale bars correspond to 1 mV. **B:** Examples of atrial preparations dissected in mice and mouse lemurs, including the sinoatrial node (SAN), the right and left atria (RA and LA, respectively). **C:** Example traces of optical action potentials (APs) recorded in the SANs of mice and mouse lemurs. APs amplitude is expressed in arbitrary units (a.u), scale bars correspond to 1 a.u. **D:** AP rate recorded in mice and mouse lemurs under the control condition (Tyrode's superfusion; n mice = 13, n mouse lemurs = 14). **E:** Dots indicating the origin of pacemaker activity in the atrial

preparations of mouse lemur hearts. **F:** Change of cardiac rate (betas or AP/min), before and after Ach or Epi, or during Epi and isoprenaline (Iso; 1 µM) and after the addition of BayK8644 (BayK; 1µM) superfusion, in Langendorff perfused hearts (n=3) or atrial preparation (n=11 in Ach, n=6 in Epi, n=5 in Iso and Iso + BayK, and n=7 in Epi and Epi + BayK) of mouse lemurs. **p<0,01, ***p<0.001 and ****p<0.0001 by unpaired T-test, two-way Anova and two-way Anova with Sidak's multi comparison test.

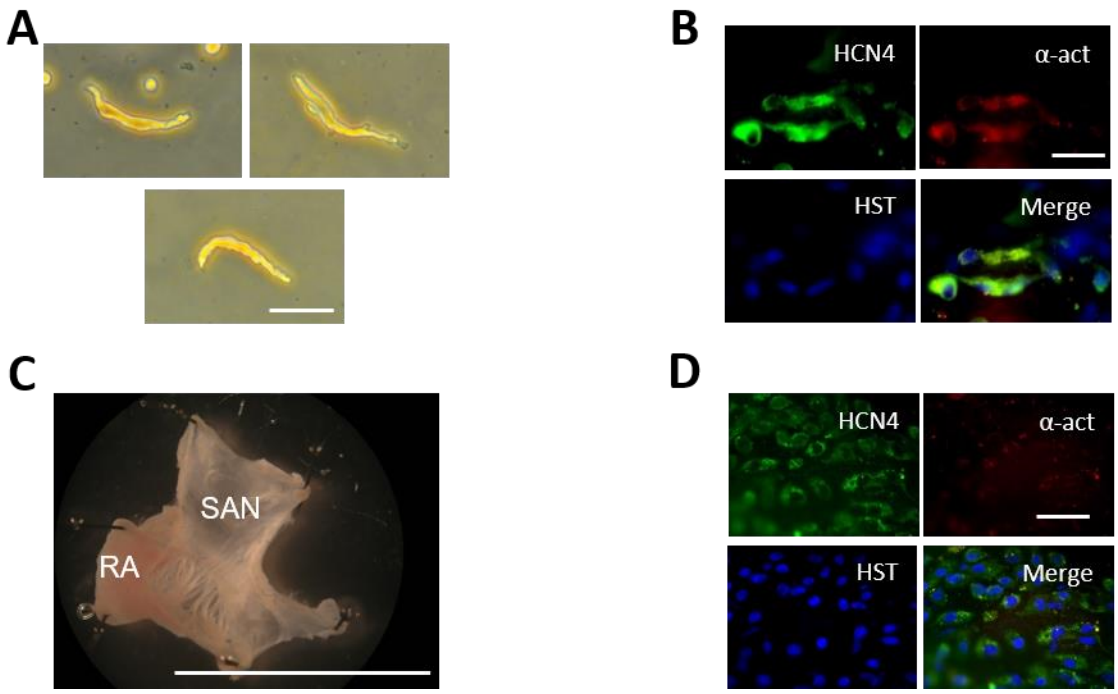

Fig 4: Immuno-detection of cardiac-pacemaker markers from mouse lemur SAN tissue and isolated myocytes.

A: Freshly isolated pacemaker myocytes obtained from mouse lemur SAN tissues (scale bar = 50 µm). **B**: Labelling of HCN4, α-actin, nuclei (Hoechst33358; HST) and merged picture in SAN pacemaker myocytes (scale bar = 30 µm). **C**) Dissection of the atrial preparation showing the SAN and the right atrium (scale bar = 10 mm). **D**) Labelling of HCN4, α-actin, nuclei (HST) and merged picture in the pacemaker myocytes within the intact SAN tissue (scale bar = 40 µm).

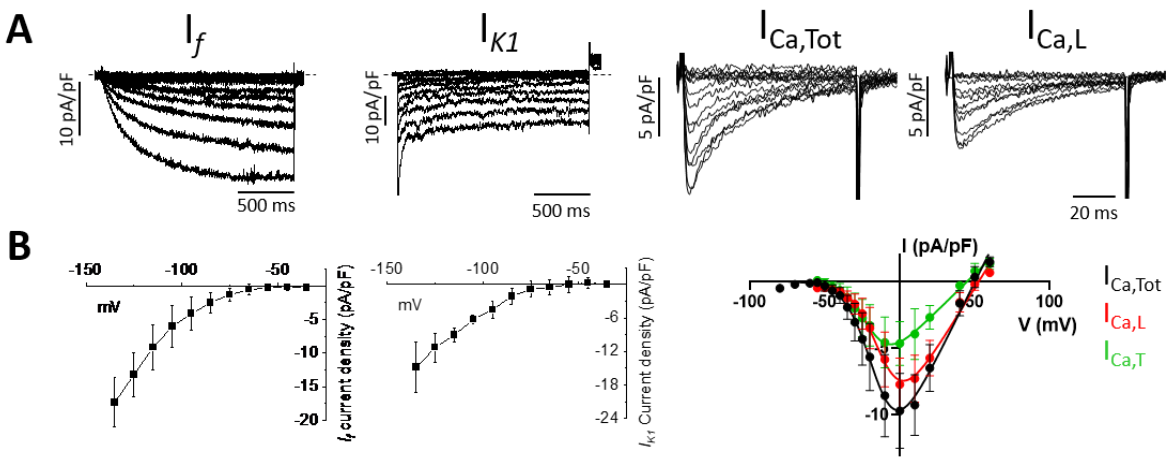

Figure 5: Recordings of ionic currents in mouse lemur pacemaker myocytes.

A: Sample traces of I_f, I_{K1}, (n = 4 and 3), and $I_{Ca,Tot}$ and $I_{Ca,L}$ (n = 4). **B:** Current-to-voltage relationships of densities of ionic currents described in panel A for I_f, I_{K1}, $I_{Ca,Tot}$, $I_{Ca,L}$ and $I_{Ca,T}$.

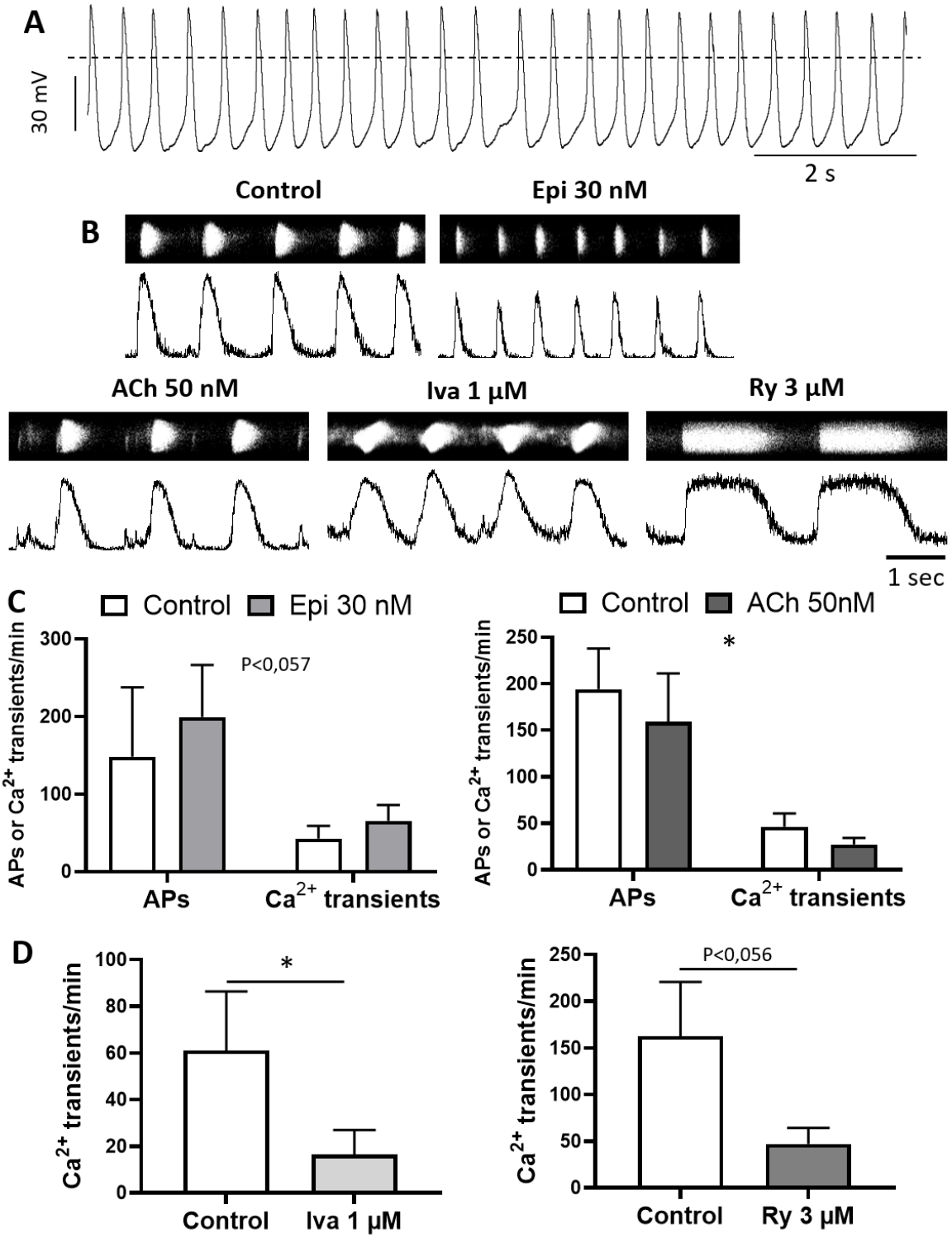

Figure 6: Patch-clamp recording of action potentials and confocal line-scan analysis of mouse lemur pacemaker myocytes.

A: Action potentials (APs) recorded in SAN pacemaker myocytes from *M. murinus* under Tyrode's superfusion. **B:** Spontaneous Ca^{2+} transients recorded in SAN pacemaker myocytes under the control condition and after perfusion of epinephrine (Epi), acetylcholine (Ach), ivabradine (Iva) and ryanodine (Ry). **C:** Effect of Epi and ACh superfusion on the rate of APs (n=2 in Epi and n=2 in Ach) and Ca^{2+} transients (n=2 in Epi and n=3 in Ach). **D:** Changes in the rate of Ca^{2+} transients after perfusion of Iva (n=4) or Ry (n=3). *p<0.05 by two-way Anova and paired T-test.

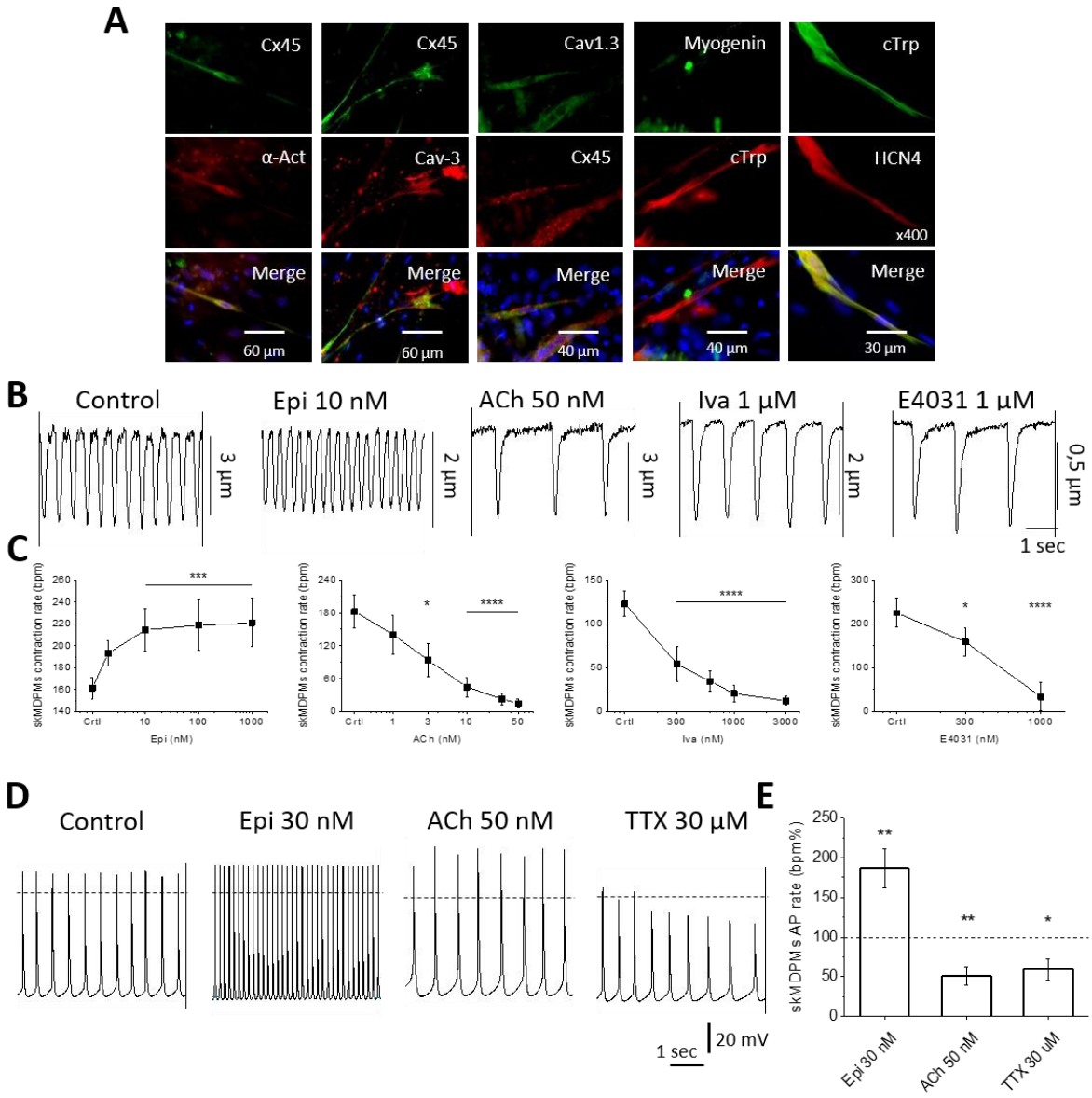

Figure 7: Automatic profile of mouse lemur PML cells.

A: Immunostaining of PML cells with the SAN marker Cx45, $Ca_v1.3$ and HCN4 plus sarcomeric alpha-actinin (α-Act), Caveolin 3 (Cav-3), myogenin and cardiac troponin I (cTrp). **B:** Example traces of cell contractions recorded in PML cells under control and after modulation with epinephrine (Epi), acetylcholine (Ach), ivabradine and E4031. **C:** Dose-response of contraction rate from PML cells under the condition in B (n = 7, 11, 9, 6 respectively). **D:** Example traces of APs recorded in PML cells under control and after modulation with epinephrine, acetylcholine and TTX. **E:** % change of spontaneous APs frequency under the conditions in D. Dashed line indicates AP rate in control conditions (n = 9, 8, 6 respectively). Paired Wilcoxon's t-tests were applied between normalized internal control and values

after drug perfusion. Two-way ANOVA/Dunnett's tests with multiple comparisons were used relative to the internal control.

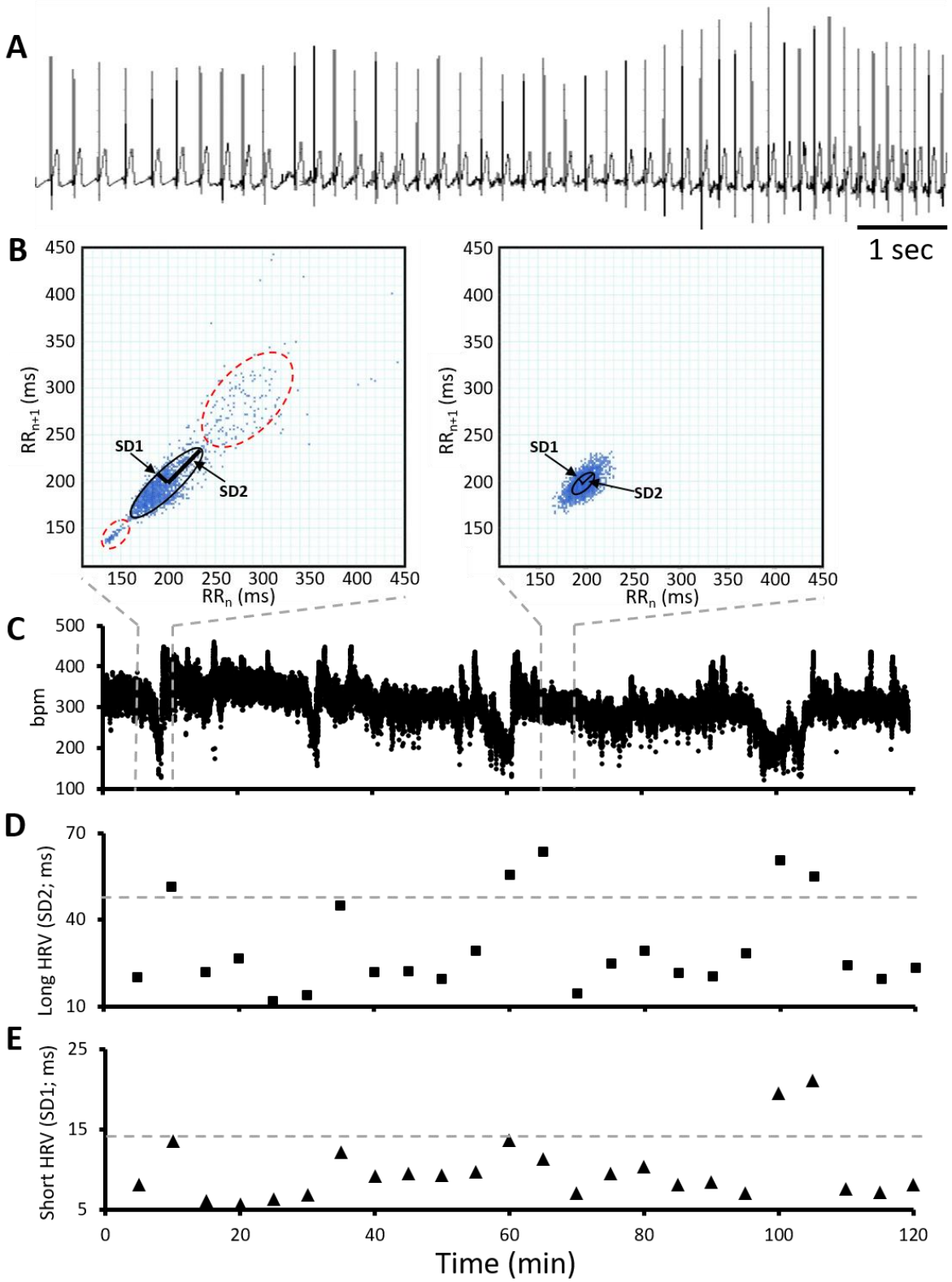

Suppl. Figure 1: Indexes of long- and short-term heart rate variability in freely moving mouse lemurs.

A: Electrocardiogram recording showing very slow heartbeats followed by a strong increase of heart rate. **B:** Poincaré plots obtained analysing intervals of 5 min during periods of high (left panel) and low (right panel) heart rate variability in C. In both panel note the standard deviations from axis 1 and 2 (SD2 and SD1, respectively) which measure short- and long -term heart rate variability (HRV). In the left panel note the presence of two clouds of points (red doted ellipses) separated from the main one (black ellipse). The points belonging to the red cloud in the upper part of the panel correspond to slow heart rate, while those belonging to the red cloud in the lower part of the panel correspond to fats heart rate. Such subdivision is absent in the right panel, which represent by Poincaré un interval of 5 min with low heart rat variability. **C:** Heart rate versus time for a period of 120 min. **D** and **E:** Plots obtained by measuring the average long- and short-term HRV (SD2 and SD1, respectively) for intervals of 5 minutes of the recording in B. Dashed gray lines in C and D indicate the threshold of mean + SD of the reported parameters.

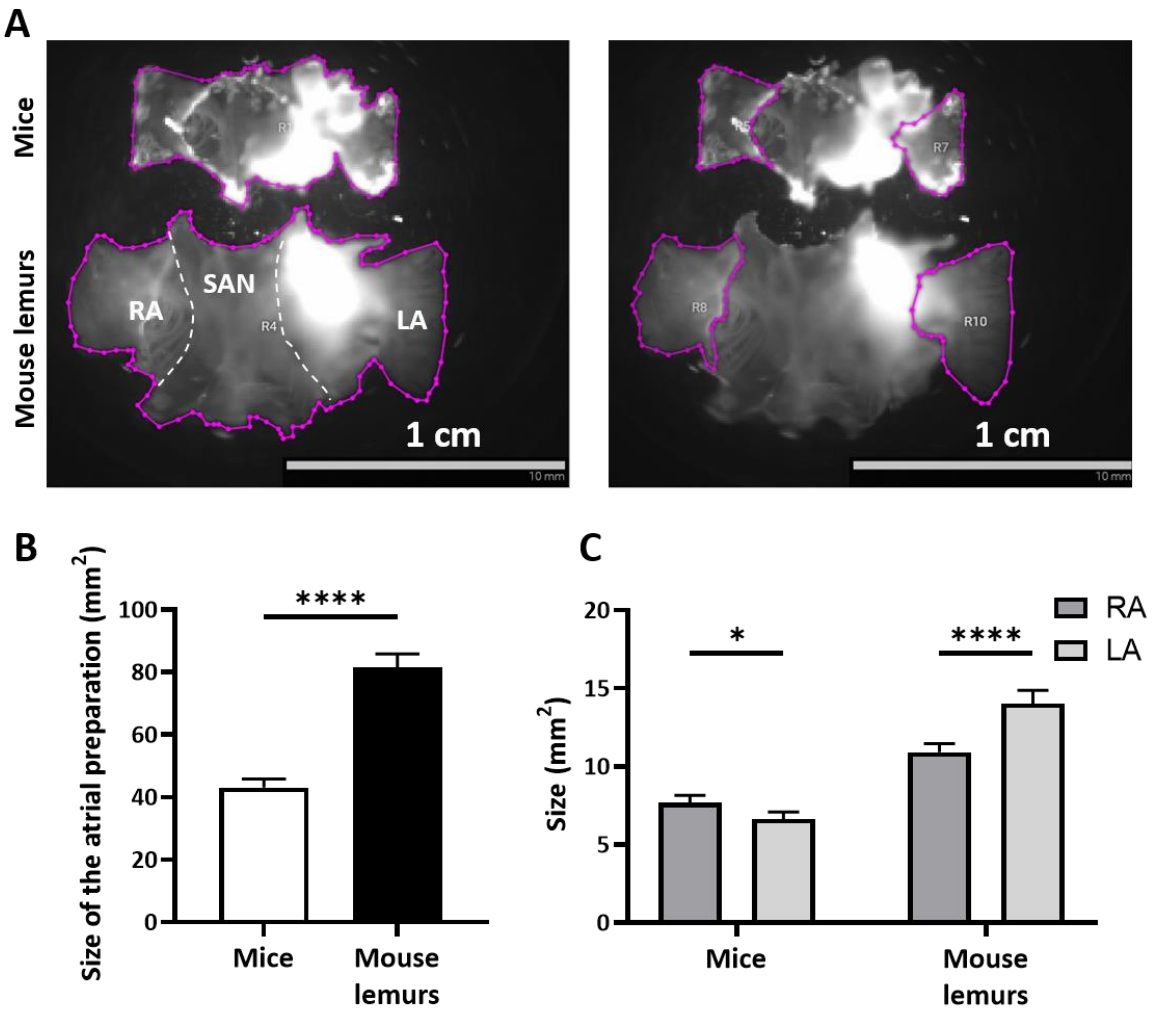

Suppl. Fig. 2: Size measurement of the atrial preparation of the heart.

A: Atrial preparations of mice and mouse lemurs including SAN, right and left atria (RA and LA, respectively). Purple lines indicate the surface of the regions constituted by the whole atrial preparation in mice and mouse lemurs (R1 and R4 respectively) the RA of mice and mouse lemurs (R5 and R8, respectively) and the LA of mice and mouse lemurs (R7 and R10, respectively). **B:** Size of the

whole atrial preparation represented in A. **C:** Size of RA and LA. N mice = 14 and n mouse lemurs = 11; *p<0.05, ****p<0.0001 by unpaired T-test and One-way Anova with Sidak's multi-comparison test.

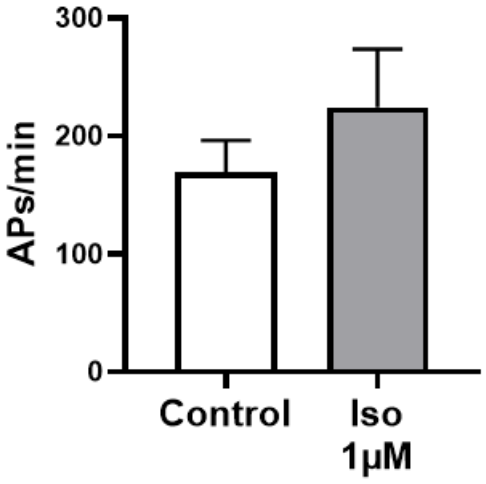

Suppl. Fig. 3: Response to saturating doses of the β-adrenergic agonist Isoprenaline (Iso).

AP rate recorded in the SAN of *M. murinus* before and after perfusion with Iso 1 µM.

Suppl. Video 1: Dynamics of pacemaker generation and conduction within the atrial preparation of mice (up) and *M. murinus* (down). Green to red colors indicated the intensity of depolarization in arbitrary units.

Bibliography

1. Irisawa, H., Brown, H. F. & Giles, W. Cardiac pacemaking in the sinoatrial node. *Physiol. Rev.* **73**, 197–227 (1993).
2. Torrente, A. G. *et al.* L-type Cav1.3 channels regulate ryanodine receptor-dependent Ca2+ release during sino-atrial node pacemaker activity. *Cardiovasc Res* **109**, 451–61 (2016).
3. Mangoni, M. E. & Nargeot, J. Genesis and regulation of the heart automaticity. *Physiol. Rev.* **88**, 919–82 (2008).
4. Mesirca, P. *et al.* The G-protein-gated K+ channel, IKACh, is required for regulation of pacemaker activity and recovery of resting heart rate after sympathetic stimulation. *J Gen Physiol* **142**, 113–26 (2013).
5. McCraty, R. & Shaffer, F. Heart Rate Variability: New Perspectives on Physiological Mechanisms, Assessment of Self-regulatory Capacity, and Health risk. *Glob Adv Health Med* **4**, 46–61 (2015).
6. Ezran, C. *et al.* The Mouse Lemur, a Genetic Model Organism for Primate Biology, Behavior, and Health. *Genetics* **206**, 651–664 (2017).
7. Dutrillaux, B. & Rumpler, Y. Chromosome banding analogies between a prosimian (Microcebus murinus), a platyrrhine (Cebus capucinus), and man. *Am J Phys Anthr.* **52**, 133–7 (1980).
8. Semelka, M., Gera, J. & Usman, S. Sick sinus syndrome: a review. *Am Fam Physician* **87**, 691–6 (2013).
9. Raatikainen, M. J. *et al.* Statistics on the use of cardiac electronic devices and electrophysiological procedures in the European Society of Cardiology countries: 2014 report from the European Heart Rhythm Association. *Europace* **17 Suppl 1**, i1-75 (2015).
10. Swaminathan, P. D. *et al.* Oxidized CaMKII causes cardiac sinus node dysfunction in mice. *J Clin Invest* **121**, 3277–88 (2011).
11. Jensen, P. N. *et al.* Incidence of and risk factors for sick sinus syndrome in the general population. *J Am Coll Cardiol* **64**, 531–8 (2014).

12. Cingolani, E., Goldhaber, J. I. & Marbán, E. Next-generation pacemakers: from small devices to biological pacemakers. *Nat Rev Cardiol* **15**, 139–150 (2018).
13. Mesirca, P., Torrente, A. G. & Mangoni, M. E. Functional role of voltage gated Ca(2+) channels in heart automaticity. *Front Physiol* **6**, 19 (2015).
14. Torrente, A. G., Mesirca, P., Bidaud, I. & Mangoni, M. E. Channelopathies of voltage-gated L-type Cav1.3/α. *Pflugers Arch* **472**, 817–830 (2020).
15. Peters, C. H., Sharpe, E. J. & Proenza, C. Cardiac Pacemaker Activity and Aging. *Annu Rev Physiol* **82**, 21–43 (2020).
16. Liang, D. *et al.* Cellular and molecular landscape of mammalian sinoatrial node revealed by single-cell RNA sequencing. *Nat Commun* **12**, 287 (2021).
17. Alings, A. M., Abbas, R. F., de Jonge, B. & Bouman, L. N. Structure and function of the simian sinoatrial node (Macaca fascicularis). *J Mol Cell Cardiol* **22**, 1453–66 (1990).
18. Billman, G. E. *et al.* Selective vagal postganglionic innervation of the sinoatrial and atrioventricular nodes in the non-human primate. *J Auton Nerv Syst* **26**, 27–36 (1989).
19. DiFrancesco, M. L., Mesirca, P., Bidaud, I., Isbrandt, D. & Mangoni, M. E. The funny current in genetically modified mice. *Prog. Biophys. Mol. Biol.* S0079610721000638 (2021) doi:10.1016/j.pbiomolbio.2021.06.003.
20. Bychkov, R. *et al.* Synchronized Cardiac Impulses Emerge From Heterogeneous Local Calcium Signals Within and Among Cells of Pacemaker Tissue. *JACC Clin Electrophysiol* **6**, 907–931 (2020).
21. Verkerk, A. O. *et al.* Pacemaker current (I(f)) in the human sinoatrial node. *Eur. Heart J.* **28**, 2472–2478 (2007).
22. Baig, S. M. *et al.* Loss of Ca(v)1.3 (CACNA1D) function in a human channelopathy with bradycardia and congenital deafness. *Nat Neurosci* **14**, 77–84 (2011).
23. Neco, P. *et al.* Paradoxical effect of increased diastolic Ca(2+) release and decreased sinoatrial node activity in a mouse model of catecholaminergic polymorphic ventricular tachycardia. *Circulation* **126**, 392–401 (2012).

24. Fischer, K. E. & Austad, S. N. The development of small primate models for aging research. *ILAR J* **52**, 78–88 (2011).

25. Bons, N., Rieger, F., Prudhomme, D., Fisher, A. & Krause, K. H. Microcebus murinus: a useful primate model for human cerebral aging and Alzheimer's disease? *Genes Brain Behav* **5**, 120–30 (2006).

26. Fritz, R. G. *et al.* Sex-specific patterns of age-related cerebral atrophy in a nonhuman primate Microcebus murinus. *Neurobiol Aging* **91**, 148–159 (2020).

27. Schmidtke, D. *et al.* Linking cognition to age and amyloid-β burden in the brain of a nonhuman primate (Microcebus murinus). *Neurobiol Aging* **94**, 207–216 (2020).

28. Lasbleiz, C. *et al.* Combining Gene Transfer and Nonhuman Primates to Better Understand and Treat Parkinson's Disease. *Front Mol Neurosci* **12**, 10 (2019).

29. Royo, J., Aujard, F. & Pifferi, F. Daily Torpor and Sleep in a Non-human Primate, the Gray Mouse Lemur (%B Front Neuroanat. **13**, 87 (2019).

30. Zhang, J. *et al.* Regulation of Torpor in the Gray Mouse Lemur: Transcriptional and Translational Controls and Role of AMPK Signaling. *Genomics Proteomics Bioinformatics* **13**, 103–10 (2015).

31. Williams, T. M. & Davis, R. W. Physiological resiliency in diving mammals: Insights on hypoxia protection using the Krogh principle to understand COVID-19 symptoms. *Comp Biochem Physiol Mol Integr Physiol* **253**, 110849 (2021).

32. Fahlman, A. *et al.* Cardiorespiratory coupling in cetaceans; a physiological strategy to improve gas exchange? *J Exp Biol* **223**, (2020).

33. Pifferi, F., Epelbaum, J. & Aujard, F. Strengths and Weaknesses of the Gray Mouse Lemur (%B Front Pharmacol. **10**, 1291 (2019).

34. Arsic, N., Mamaeva, D., Lamb, N. J. & Fernandez, A. Muscle-derived stem cells isolated as non-adherent population give rise to cardiac, skeletal muscle and neural lineages. *Exp. Cell Res.* **314**, 1266–1280 (2008).

35. Mesirca, P. *et al. Bradycardic mice undergo effective heart rate improvement after specific homing to the sino-atrial node and differentiation of adult muscle derived stem cells*. https://doi.org/10.1101/393512 (2018) doi:10.1101/393512.
36. Konopelski, P. & Ufnal, M. Electrocardiography in rats: a comparison to human. *Physiol Res* **65**, 717–725 (2016).
37. Mesquita, T. R. R. *et al.* Mechanisms of atrial fibrillation in aged rats with heart failure with preserved ejection fraction. *Heart Rhythm* **17**, 1025–1033 (2020).
38. Mertens, A., Stiedl, O., Steinlechner, S. & Meyer, M. Cardiac dynamics during daily torpor in the Djungarian hamster (Phodopus sungorus). *Am J Physiol Regul Integr Comp Physiol* **294**, R639-50 (2008).
39. Nerbonne, J. M., Nichols, C. G., Schwarz, T. L. & Escande, D. Genetic manipulation of cardiac K(+) channel function in mice: what have we learned, and where do we go from here? *Circ Res* **89**, 944–56 (2001).
40. Mesirca, P. *et al.* G protein-gated IKACh channels as therapeutic targets for treatment of sick sinus syndrome and heart block. *Proc Natl Acad Sci U A* **113**, E932-41 (2016).
41. Baudot, M. *et al.* Concomitant genetic ablation of L-type Ca. *Sci Rep* **10**, 18906 (2020).
42. Torrente, A. G. *et al.* Burst pacemaker activity of the sinoatrial node in sodium-calcium exchanger knockout mice. *Proc Natl Acad Sci U A* **112**, 9769–74 (2015).
43. Shinagawa, Y., Satoh, H. & Noma, A. The sustained inward current and inward rectifier K+ current in pacemaker cells dissociated from rat sinoatrial node. *J Physiol* **523 Pt 3**, 593–605 (2000).
44. Cho, H., Takano, M. & Noma, A. The Electrophysiological Properties of Spontaneously Beating Pacemaker Cells Isolated from Mouse Sinoatrial Node. *J. Physiol.* **550**, 169–180 (2003).
45. Mangoni, M. E. & Nargeot, J. Properties of the hyperpolarization-activated current (I(f)) in isolated mouse sino-atrial cells. *Cardiovasc Res* **52**, 51–64 (2001).

46. Mangoni, M. E. *et al.* Functional role of L-type Cav1.3 Ca2+ channels in cardiac pacemaker activity. *Proc. Natl. Acad. Sci. U. S. A.* **100**, 5543–8 (2003).

47. Mamaeva, D. *et al.* Novel roles for voltage-gated T-type Ca $^{2+}$ and ClC-2 channels in phagocytosis and angiogenic factor balance identified in human iPSC-derived RPE. *FASEB J.* **35**, (2021).

48. Zohdy, S. *et al.* Teeth, sex, and testosterone: aging in the world's smallest primate. *PloS One* **9**, e109528 (2014).

49. Prabhakar, H. & Kapoor, I. *Brain and heart crosstalk*. (Springer, 2020).

50. Steenman, M. & Lande, G. Cardiac aging and heart disease in humans. *Biophys. Rev.* **9**, 131–137 (2017).

51. Baudot, M. *et al.* Concomitant genetic ablation of L-type Ca. *Sci Rep* **10**, 18906 (2020).

52. Lakatta, E. G., Maltsev, V. A. & Vinogradova, T. M. A coupled SYSTEM of intracellular Ca2+ clocks and surface membrane voltage clocks controls the timekeeping mechanism of the heart's pacemaker. *Circ. Res.* **106**, 659–73 (2010).

53. Hozer, C., Perret, M., Pavard, S. & Pifferi, F. Survival is reduced when endogenous period deviates from 24 h in a non-human primate, supporting the circadian resonance theory. *Sci. Rep.* **10**, 18002 (2020).

54. Mangoni, M. E., Marger, L. & Nargeot, J. If current inhibition: cellular basis and physiology. *Adv Cardiol* **43**, 17–30 (2006).